Published in final edited form as:
Science. 2020 October 30; 370(6516): 550–557. doi:10.1126/science.aba3178.

Receptor kinase module targets PIN-dependent auxin transport during canalization

Jakub Hajný[1,2], **Tomáš Prát**[1], **Nikola Rydza**[3], **Lesia Rodriguez**[1], **Shutang Tan**[1], **Inge Verstraeten**[1], **David Domjan**[1], **Ewa Mazur**[3,4], **Elwira Smakowska-Luzan**[5,9], **Wouter Smet**[6,7], **Eliana Mor**[6,7], **Jonah Nolf**[6,7], **BaoJun Yang**[6,7], **Wim Grunewald**[6,7], **Gergely Molnár**[1,8], **Youssef Belkhadir**[9], **Bert De Rybel**[6,7], **Jiří Friml**[1,*]

[1]Institute of Science and Technology (IST), 3400 Klosterneuburg, Austria [2]Laboratory of Growth Regulators, The Czech Academy of Sciences, Institute of Experimental Botany & Palacký University, Šlechtitelů 27, CZ-78371 Olomouc, Czech Republic [3]Mendel Centre for Plant Genomics and Proteomics, Central European Institute of Technology (CEITEC), Masaryk University, Brno, Czechia [4]Department of Cell Biology, Faculty of Biology and Environmental Protection, University of Silesia in Katowice, Jagiellońska 28, 40-032 Katowice, Poland [5]Laboratory of Biochemistry, Wageningen University, Stippeneng 4, 6708 Wageningen, the Netherlands [6]Ghent University, Department of Plant Biotechnology and Bioinformatics, 9052 Ghent, Belgium [7]VIB Center for Plant Systems Biology, 9052 Ghent, Belgium [8]Department of Applied Genetics and Cell Biology, University of Natural Resources and Life Sciences, (BOKU), Vienna, Austria [9]Gregor Mendel Institute (GMI), Austrian Academy of Sciences, Vienna Biocenter (VBC), Vienna, Austria

Abstract

Spontaneously arising channels transporting the phytohormone auxin provide positional cues for self-organizing aspects of plant development such as flexible vasculature regeneration or its patterning during leaf venation. The auxin canalization hypothesis proposes a feed-back between auxin signaling and transport as underlying mechanism but molecular players await discovery. Here we identified part of the machinery that routes auxin transport. The auxin-regulated receptor CAMEL (Canalization-related, Auxin-regulated Malectin-type RLK) together with CANAR (Canalization-related Receptor-like kinase) interact with and phosphorylate PIN auxin transporters. *camel* and *canar* mutants are impaired in PIN1 subcellular trafficking and auxin-mediated PIN polarization, which macroscopically manifests as defects in leaf venation and vasculature regeneration after wounding. The CAMEL-CANAR receptor complex is part of the auxin feed-back that coordinates polarization of individual cells during auxin canalization.

*Correspondence to: Jiří Friml, Institute of Science and Technology Austria (IST Austria), Am Campus 1, A-3400 Klosterneuburg (Austria), Tel: +43 (0)2243 9000 5401, Fax: +43 (0)2243 9000 2000, jiri.friml@ist.ac.at.

Author contributions: J.F. and W.G. conceived and designed the experiments. J.H. and J.F. wrote the paper with help of B.R. and Y.B. J.H., T.P., L.R., S.T., I.V., D.D., N.R., E.M., E.S.L., W.S., E.M., B.Y., B.D.R., Y.B., J.N. conducted experiments and contributed to the study design. G.M., J.H. and I.V., analyzed the data.

Competing interests: The authors declare that they have no competing interests.

Europe PMC Funders Author Manuscripts

Introduction

Plant development flexibly adapts the plant's architecture and physiology to an ever-changing environment. Much of this adaptive development is characterized by self-organization of patterning processes, such as integration of new organs with the pre-existing vascular network, rise of complex leaf processes, such as integration of new organs with the pre-existing vascular network, rise of complex leaf venation patterns and flexible vasculature regeneration around the wound.

Formation of organized vasculature from originally uniform tissues involves coordinated polarization of individual cells. Canalization hypothesis proposes that the plant hormone auxin acts as a polarizing cue by means of its directional intercellular flow and the feed-back between auxin signaling and transport (1). Auxin transport is mediated by polarly localized PIN auxin transport proteins (2) and thus auxin signaling coordinating the repolarization of PINs in individual cells can generate auxin transport channels demarcating the future position of forming vasculature. The emergence of PIN-expressing auxin channels preceding vasculature formation has been observed in different plant species connecting newly formed organs (3) or lateral shoot branches (4) with pre-existing vasculature network, also during leaf venation (5), in embryogenesis (6) and during regeneration after wounding (7, 8). Similar PIN-expressing auxin channels arise from an artificial local auxin source revealing that auxin is the necessary and sufficient signal for channel formation (4, 8).

It remains enigmatic how such auxin feed-back on subcellular PIN localization leading to coordinated tissue polarization can integrate directional and positional cues. Auxin transcriptionally regulates *PIN* expression (9) and inhibits PIN endocytic recycling (10), which may explain auxin-mediated PIN repolarization by *de novo* secretion and by a differential endocytosis rate of PIN proteins from the plasma membrane leading to establishment of polarity (11). A mechanistic model of auxin canalization (12) predicts that PIN polarization away from the auxin source can arise from a combination of intracellular, transcriptional auxin signaling regulating PIN abundance and cell surface auxin signaling regulating PIN internalization rate (10) and thereby stabilizing PINs at the given cell side. This mechanism would sense an auxin gradient throughout the tissue and translate it into tissue polarization. Additionally, a so far elusive short-range signaling mechanism would mediate coordination between individual cells during this process.

Here, we identified a CAMEL-CANAR cell surface receptor complex, acting downstream of the canonical TIR1/AFB-WRKY23 auxin signaling, which is required for the auxin effect on PIN trafficking and polarity in individual cells as well as for coordinated tissue polarization during vascular formation and regeneration.

Results

Identification of potential auxin canalization regulators downstream of WRKY23

To gain more insight into the auxin regulation of PIN polarity, we designed a microarray experiment to find genes downstream of the *WRKY DNA-BINDING Protein 23* (*WRKY23)* transcription factor that regulates auxin-mediated PIN repolarization (13) (Fig. S1A,B). We

obtained 14 genes as auxin-inducible, potential targets of WRKY23 (Fig. 1A; Tab. S1). To identify among them regulators of auxin canalization, we isolated or used previously described corresponding loss-of-function mutants. We analyzed the vasculature formation during leaf development as a classical process requiring auxin feedback on PIN-dependent auxin transport (5). Typically, wild type (Wt) cotyledons form a conserved pattern of four loops as in most mutants with exception of mutants in AT5G40780 and AT1G05700, where we observed strong venation defects: (Fig. S1C; AT5G40780/*lht1-1*: 41% and AT1G05700/*camel-1*: 45%; where % stands for any type of abnormality deviating from typical Wt pattern).

Thus, we identified AT5G40780 and AT1G05700 acting downstream of TIR1/AFB-WRKY23 and being required for canalization-based processes such as leaf venation.

Malectin-type LRR Receptor-like kinase CAMEL downstream of auxin signaling

AT1G05700 encodes a previously uncharacterized member of the Leucine-Rich Repeat (LRR) receptorlike kinase (RLK) family from the subfamily I and its extracellular domain consists of a large Malectin-like domain and three LRR repeats (Fig. 1C; Fig. S1D). We named AT1G05700 CAMEL (Canalization-related Auxin-dependent Malectin-like RLK).

qRT-PCR on lines where *WRKY23* is either targeted inducibly to the nucleus (*35S::WRKY23-GR*) or engineered into a transcriptional repressor (*35S::WRKY23-SRDX*) (14) confirmed that *CAMEL* mRNA levels increased after activation of WRKY23 and decreased after its repression (Fig. 1D). The JASPAR database of transcription factors (TFs) (15) also predicted WRKY23 among the top candidates binding to a 2000bp *CAMEL* promoter (Tab. S2). We confirmed an activation of *CAMELpro* by WRKY23 using the luciferase-based reporter system in *Nicotiana benthamiana*. A co-expression of *35S::WRKY23* and *CAMELpro::LUC* led to activation of luciferase activity (Fig. 1F). This supports that *CAMEL* is a downstream gene of WRKY23.

As shown previously, the TIR1/AFB auxin pathway is required for auxin-mediated PIN polarity re-arrangements and canalization-based development (4, 8) and this goes in part through *WRKY23* (13). Consistently with this, *CAMEL* transcription, similar to *WRKY23,* is induced by auxin in a time- and dose-dependent manner (Fig. S1E,F) and this auxin effect is not observed in *35S::WRKY23-SRDX* line or in mutants defective in transcriptional auxin signaling (*HS::axr3-1* and *arf7arf19*) (Fig. 1D,E). Furthermore, *CAMELpro* contains 6 auxin responsive elements (Fig. S1G), suggesting additional auxin regulation, possibly directly by ARFs, also supported by fast upregulation of *CAMEL* by auxin (Fig. S1F).

Thus, *CAMEL* is transcriptionally regulated by WRKY23 downstream of the TIR1/AFB-ARF signaling module.

CAMEL-CANAR signaling complex at the cell surface

To identify other receptor-like kinases that might interact with CAMEL, we used a map of physical interactions between extracellular domains of *Arabidopsis* LRR-RLKs (16). A large class VII LRR-RLK was retrieved as a single, high-confidence interactor (Fig. 1B,C; Fig.

S1H). Given its association with CAMEL in canalization processes, we named it CANAR (Canalization-related Receptor-like kinase).

To determine whether CAMEL and CANAR interact *in vivo* as full-length proteins we used three approaches. Firstly, we immunoprecipitated CANAR-GFP using anti-GFP antibodies and performed tandem mass spectrometry to identify proteins co-immunoprecipitated with our bait. We obtained a list with possible interactors including CAMEL among the top 10 interactors (Tab. S3). Next, we tested the CAMEL-CANAR interaction using bimolecular fluorescence complementation (BiFC) in *Nicotiana benthamiana* leaves. Co-infiltration of *CAMEL* and *CANAR* resulted in a positive signal in both combinations (35S::CAMEL-(C)CFP + 35S::CANAR-(N)CFP and *vice versa*). A negative control 35S::TMK2(C)CFP + 35S::CANAR(N)CFP did not show a signal (Fig. S1I).

To test the CAMEL-CANAR interaction more quantitatively, we used Förster resonance energy transfer combined with fluorescence lifetime imaging microscopy (FRET-FLIM). We co-expressed *35S::CANAR-GFP* and *35S::CAMEL-mCherry* in *Arabidopsis* root protoplasts and detected a reduction in the GFP fluorescence life time as compared to *35S::CANAR-GFP* expressed alone (Fig. 1G,H). Auxin treatment had no effect on CAMEL-CANAR interaction. Spatial resolution of FRET-FLIM experiments suggested that both proteins are localized and form complexes at the cell surface (Fig.1G).

These observations showed constitutive, auxin-insensitive interaction between CAMEL and CANAR.

CAMEL and CANAR in leaf venation

Next, we tested genetically an involvement of CAMEL-CANAR complex in auxin-mediated canalization. We isolated publicly available T-DNA insertional loss-of-function mutants in both genes: *camel-1/-2* and *canar-1/-2* (Fig. S2A-D), and generated gain-of-function transgenic lines overexpressing *CAMEL* and *CANAR* under the constitutive *RPS5A* and *35S* promoters, respectively (Fig. S2E,F).

The *camel-1/-2* mutants showed abnormal vascular patterning with disconnected upper loops, extra branches and extra or missing loops. Two independent overexpression lines also exhibited vasculature defects albeit with lesser frequency (Fig. 2A,B). Also both *canar-1/-2* mutant alleles showed similar, even more pronounced vasculature abnormalities whereas *35S::CANAR-GFP* exhibited overall less frequent defects (Fig. 2C,D). Double mutant *camel-1xcanar-1* exhibited largely rescued venation implying a possible antagonistic action of CAMEL and CANAR (Fig. 2A,C; S2G). CAMEL/CANAR function appears to be rather specific to vasculature formation as no other obvious growth defects were observed (Fig. S2H-P).

Next, we tested if these venation defects are linked to altered auxin distribution and auxin transport. We analyzed the expression of the auxin-responsive reporter *DR5rev::GFP*, which can be correlated with auxin distribution (17). In both *camel-1* and *canar-1* mutants DR5 activity was decreased compared to the control (Fig. 2E,F). When analyzing the basipetal (rootward) auxin transport in hypocotyls, we observed that both *camel-1* and *canar-1*

mutants have reduced auxin flow (Fig. S2Q). Given that formation of PIN1-expressing, polarized channels has been linked to vein formation (5) we examined PIN1 polarity in young first leaves by means of anti-PIN1 antibody staining. In Wt leaves, coordinated PIN1 polarity defining auxin-transporting channel was observed with rare PIN1 polarity abnormalities in primary and secondary branches. In contrast, both *camel-1* and *canar-1* mutants showed higher incidence of PIN1 polarity defects (marked by red arrows) in primary and *canar-1* also in secondary branches (Fig. 2G,H) whereas no defects were observed in midvein for any tested genotypes (Fig. S2R).

These observations show that the CAMEL and CANAR mediate vasculature development during leaf venation and coordinate PIN1 polarities during this process.

CAMEL and CANAR in vasculature regeneration after wounding

Another classical example of a canalization-mediated process is vasculature regeneration after wounding when new vasculature is generated circumventing the wound (7, 8).

We interrupted the vasculature in the *Arabidopsis thaliana* inflorescence stem by a horizontal cut (Fig. 3A) and analyzed GUS expression at 1-7 days after wounding (DAW). Both *CAMEL* and *CANAR* as well as their upstream regulator *WRKY23* showed promoter activities during the regeneration (Fig. 3B; S3A). Next, we analyzed the extent of vasculature regeneration in loss-of-function mutants and overexpressing lines as visualized by toluidine blue staining (TBO) of regenerated vasculature. In Wt, vasculature was fully developed and both newly regenerated vessel cells (white asterisk) and lignified parenchyma cells (red asterisk) stained in blue were visible. All tested mutants showed defective regeneration caused by inability to form a continuous strand of regenerated cells. *RPS5A::CAMEL* showed less frequent defects and *35S::CANAR-GFP* exhibited even improved regeneration over the Wt (Fig. 3C,D; S3B,C). Similar defects were observed also for flexible formation of auxin transport channels. In *PIN1*-GFP line, but not in *canar-1xPIN1-GFP*, PIN1-GFP expressing channel (marked by yellow arrow) circumventing the wound was formed (Fig. S3D). In contrast to leaf venation, *camel-1xcanar-1* double mutant showed regeneration defects comparable to individual mutants (Fig. S3B,C).

To analyze more directly auxin-mediated formation of auxin transport channels, we used external, local auxin application (18). Application of IAA droplet on the stem side below the wound (marked by magenta) led to formation of PIN1-expressing channel connecting with the pre-existing vasculature already after 2 DAW in Wt, an effect not observed in *canar-1* background even after 4 DAW (Fig. S3E). Accordingly, the similar, newly formed vascular strands (as revealed by TBO staining) could be observed only in Wt (Fig. S3F).

These results revealed a role for CAMEL and CANAR as well as their upstream regulator WRKY23 in the flexible regeneration of vasculature following wounding.

CAMEL and CANAR in trafficking and polarity of PIN auxin transporters

Since auxin feed-back on PIN polarity is one of the main features of canalization and PIN polar localization is linked to its constitutive endocytic recycling (11, 12) we tested whether CAMEL and CANAR are involved in these processes. PIN endocytic recycling can be

indirectly visualized by PIN intracellular aggregation in response to treatment with the trafficking inhibitor Brefeldin A (BFA) (19). Anti-PIN1 immunostaining in roots showed that following BFA treatment, PIN1 intracellular aggregation was reduced in *camel-1* and *canar-1* mutants (Fig. 4A,B). The same phenomenon was observed for *camel-1xPIN2-GFP* and *canar-1xPIN2-GFP* crosses (Fig. S4A,B) indicating a defect in the PIN endocytic recycling.

The auxin effect on PIN polarity can be approximated by the repolarization of PIN1 from the basal to the inner lateral side in the root endodermis cells (8). Anti-PIN1 immunolocalization revealed that following auxin treatment, PIN1 repolarization was reduced in *camel* and *canar* mutants (Fig. 4C,D; S4C-E).

These results imply that the CAMEL-CANAR complex not only plays a role in the canalization-related development at the level of organs and tissues but also targets PIN1 in individual cells, regulating its subcellular trafficking and auxin feed-back on PIN polarity.

CAMEL-CANAR receptor complex targets and phosphorylates PIN auxin transporters

To get insight into the mechanism of CAMEL-CANAR action and downstream processes, we immunoprecipitated CAMEL-GFP from seedlings to identify the interactome of CAMEL. Co-immunoprecipitated proteins were pulled-down and analyzed using mass spectrometry (Tab. S4). Among the list of putative interactors multiple PIN proteins were found.

To confirm the interaction with PIN1, we transiently co-expressed *35S::CAMEL-GFP +35S::PIN1-mRFP* and *35S::CANAR-GFP+35S::PIN1-mRFP* in *Arabidopsis* root protoplasts. PIN1-mRFP co-immunoprecipitated with both CANAR-GFP and CAMEL-GFP (Fig. 5A). Furthermore, we performed FRET-FLIM in root protoplasts expressing *35S::CAMEL-GFP* or *35S::CANAR-GFP*. The lifetime of CAMEL-GFP and CANAR-GFP was reduced after co-expression with $PIN1^{HL}$-mCherry (HL=hydrophilic loop) further confirming an interaction between CAMEL/CANAR and PIN1 (Fig. 5B,C).

Since CAMEL and CANAR are expected to act as kinases and PIN phosphorylation is a well-established mode of regulation of PIN activity and polar localization (2), we tested the ability of CAMEL and CANAR to phosphorylate PINs. We therefore performed an *in vitro* kinase assay by incubating purified $PIN1^{HL}$, $PIN2^{HL}$ or $PIN3^{HL}$ with purified cytoplasmic kinase domains of CAMEL and CANAR with radiolabeled ATP. We detected phosphorylation of PIN loops by CAMEL with $PIN1^{HL}$ being the best substrate (Fig. 5D). However, CANAR did not show kinase activity (Fig. S5A). Lack of kinase activity can be explained by losing an aspartic acid from the conserved HRD motif in the catalytic core similarly to other known pseudokinases: BIR2, GHR1, PRK5 (Fig. S5B).

Considering the lack of CANAR kinase activity, constitutive CAMEL-CANAR interaction and complementation of leave vasculature defects of *camel-1xcanar-1* double mutant, we hypothesize that CANAR might be a negative regulator of CAMEL. This is further supported by ability of CANAR kinase domains to reduce CAMEL auto-phosphorylation and kinase activity towards PIN1 (Fig. S5C).

To test relevance of CAMEL-mediated PIN1 phosphorylation, we analyzed *in vitro* kinase reaction using mass spectrometry and identified five mostly conserved putative phosphosites in PIN1^{HL} (Fig. S5D; 6A-C). These sites seem unique since they are not shared by any previously reported kinase phosphorylating PIN loop such as PID/WAGs, D6PK or MPKs (Fig. S5D) and when mutated, they decreased the ability of CAMEL kinase domain to phosphorylate PIN1^{HL} (Fig. S6A,B).

We generated phosphodead *PIN1-GFP^{T3AS2A}* and phosphomimic *PIN1-GFP^{T3ES2E}* constructs by substitution of three threonine and two serine to alanine or glutamic acid, respectively, placed them under control of the native *PIN1* promoter and introduced into Wt plants. Positive, GFP-expressing transformants for both constructs showed already in the first generation naked inflorescence stems (7/20 for *PIN1-GFP^{T3AS2A}* and 3/18 for *PIN1-GFP^{T3ES2E}*) strongly reminiscent of *pin1* loss-of-function (Fig. 6B). Other positive plants did not show strong phenotypes and produced seeds allowing analysis in the next generation. Venation in cotyledons of both *PIN1-GFP^{T3AS2A}* and *PIN1-GFP^{T3ES2E}* lines exhibited increased incidence of vascular abnormalities (Fig. 6D,E; S6C). All positive transformants in the first generation for *PIN1^{T3AS2A}* (4/4) and *PIN1^{T3ES2E}* (2/2) showing naked inflorescence stems exhibited no vasculature regeneration after wounding characterized by fragmented vessel cells, non-functional parenchyma cell connections or extensive callus formation in the wound (Fig. S6E). To test the role of the identified phosphosites in canalization, we tested auxin effect on mutated PIN1 variants. While PIN1-GFP is localized in roots predominantly basal, both PIN1-GFP^{T3AS2A} and PIN1-GFP^{T3ES2E} showed more apolar localization already without any treatments (Fig. 6C; S6D). When immunolocalized with anti-GFP antibody, both PIN1-GFP^{T3AS2A} and PIN1-GFP^{T3ES2E} already partially polarized to the inner-lateral side in the mock situation, did not show any further polarity changes following auxin application (Fig. 6F; S6D).

In conclusion, the CAMEL-CANAR complex interacts with PINs and CAMEL is capable of phosphorylating their cytosolic loops. Effects of phosphomimic and phosphodead mutations in the PIN1 loop support the relevance of these phosphorylations for auxin transport and auxin canalization. The stronger defects in lines carrying PIN1 with mutated CAMEL-targeted phosphorylation sites as compared to the *camel/canar* mutants suggest that these phosphosites are shared by other kinases controlling auxin transport in a different developmental contexts.

Discussion

In this study, we provided mechanistic insights into how auxin controls its own directional cell-to-cell transport and identified molecular components of so-called auxin canalization mechanism underlying flexible and self-organizing formation of auxin channels guiding vasculature formation. Identification of CAMEL-CANAR complex downstream of transcriptional auxin signaling and its direct regulation of PIN-dependent auxin transport provide a potential means how to integrate global auxin signals with a so far hypothetical short range signaling for coordinating cell polarities during plant adaptive development.

Europe PMC Funders Author Manuscripts

Supplementary Material

Refer to Web version on PubMed Central for supplementary material.

Acknowledgements

We would like to acknowledge M. Glanc and Y. Zhang for providing entry clones; Vienna Biocenter Core Facilities (VBCF) for recombinant protein production and purification; Vienna Biocenter Mass spectrometry Facility, Bioimaging and Life Science Facilities at IST Austria and Proteomics Core Facility CEITEC for a great assistance.

Funding

This project received funding from the European Research Council (ERC) under the European Union's Horizon 2020 research and innovation program (grant agreement No 742985) and Austrian Science Fund (FWF): I 3630-B25 to J.F; the Austrian Agency for International Cooperation in Education & Research to D.D.; W.S. was funded by the Netherlands Organization for Scientific Research (NWO; VIDI-864.13.001); the Research Foundation - Flanders (FWO; Odysseus II G0D0515N) and a European Research Council grant (ERC; StG TORPEDO; 714055) to B.D.R., B.Y. and E.M.; the Hertha Firnberg Programme post-doctoral fellowship (T-947) from the FWF Austrian Science Fund to E.S.-L.. J.H. is Recipient of a DOC Fellowship of the Austrian Academy of Sciences at IST Austria.

Data and materials availability

All data is available in the main text or the supplementary materials. Raw microarray data from this article can be found in the EMBL ArrayExpress repository under accession number: XXXX.

References and Notes

1. Berleth T, Sachs T. Plant morphogenesis: long-distance coordination and local patterning. Curr Opin Plant Biol. 2001; 4:57–62. [PubMed: 11163169]
2. Adamowski M, Friml J. PIN-Dependent Auxin Transport: Action, Regulation, and Evolution. Plant Cell Online. 2015; 27:20–32.
3. Benková E, Michniewicz M, Sauer M, Teichmann T, Seifertová D, Jürgens G, Friml J. Local, Efflux-Dependent Auxin Gradients as a Common Module for Plant Organ Formation. Cell. 2003; 115:591–602. [PubMed: 14651850]
4. Balla J, Kalousek P, Reinöhl V, Friml J, Procházka S. Competitive canalization of PIN-dependent auxin flow from axillary buds controls pea bud outgrowth. Plant J. 2011; 65:571–577. [PubMed: 21219506]
5. Scarpella E, Marcos D, Friml J, Berleth T. Control of leaf vascular patterning by polar auxin transport. Genes Dev. 2006; 20:1015–1027. [PubMed: 16618807]
6. Robert HS, Grones P, Stepanova AN, Robles LM, Lokerse AS, Alonso JM, Weijers D, Friml J. Local auxin sources orient the apical-basal axis in Arabidopsis embryos. Curr Biol CB. 2013; 23:2506–2512. [PubMed: 24291089]
7. Mazur E, Benková E, Friml J. Vascular cambium regeneration and vessel formation in wounded inflorescence stems of Arabidopsis. Sci Rep. 2016; 6doi: 10.1038/srep33754
8. Sauer M, Balla J, Luschnig C, Wiśniewska J, Reinöhl V, Friml J, Benková E. Canalization of auxin flow by Aux/IAA-ARF-dependent feedback regulation of PIN polarity. Genes Dev. 2006; 20:2902–2911. [PubMed: 17043314]
9. Vieten A, Vanneste S, Wisniewska J, Benkova E, Benjamins R, Beeckman T, Luschnig C, Friml J. Functional redundancy of PIN proteins is accompanied by auxin-dependentcross-regulation of PIN expression. Development. 2005; 132:4521–4531. [PubMed: 16192309]
10. Paciorek T, Zazímalová E, Ruthardt N, Petrásek J, Stierhof Y-D, Kleine-Vehn J, Morris DA, Emans N, Jürgens G, Geldner N, Friml J. Auxin inhibits endocytosis and promotes its own efflux from cells. Nature. 2005; 435:1251–1256. [PubMed: 15988527]

11. Glanc M, Fendrych M, Friml J. Mechanistic framework for cell-intrinsic re-establishment of PIN2 polarity after cell division. Nat Plants. 2018; 4:1082–1088. [PubMed: 30518833]
12. Wabnik K, Kleine-Vehn J, Balla J, Sauer M, Naramoto S, Reinöhl V, Merks RMH, Govaerts W, Friml J. Emergence of tissue polarization from synergy of intracellular and extracellular auxin signaling. Mol Syst Biol. 2010; 6doi: 10.1038/msb.2010.103
13. Prát T, Hajný J, Grunewald W, Vasileva M, Molnár G, Tejos R, Schmid M, Sauer M, Friml J. WRKY23 is a component of the transcriptional network mediating auxin feedback on PIN polarity. PLOS Genet. 2018; 14
14. Grunewald W, De Smet I, Lewis DR, Löfke C, Jansen L, Goeminne G, Bossche RV, Karimi M, De Rybel B, Vanholme B. Transcription factor WRKY23 assists auxin distribution patterns during Arabidopsis root development through local control on flavonol biosynthesis. Proc Natl Acad Sci. 2012; 109:1554–1559. [PubMed: 22307611]
15. Khan A, Fornes O, Stigliani A, Gheorghe M, Castro-Mondragon JA, van der Lee R, Bessy A, Chèneby J, Kulkarni SR, Tan G, Baranasic D, et al. JASPAR 2018: update of the open-access database of transcription factor binding profiles and its web framework. Nucleic Acids Res. 2018; 46:D260–D266. [PubMed: 29140473]
16. Smakowska-Luzan E, Mott GA, Parys K, Stegmann M, Howton TC, Layeghifard M, Neuhold J, Lehner A, Kong J, Grünwald K, Weinberger N, et al. An extracellular network of *Arabidopsis* leucine-rich repeat receptor kinases. Nature. 2018; 553:342. [PubMed: 29320478]
17. Friml J, Vieten A, Sauer M, Weijers D, Schwarz H, Hamann T, Offringa R, Jürgens G. Efflux-dependent auxin gradients establish the apical–basal axis of Arabidopsis. Nature. 2003; 426:147–153. [PubMed: 14614497]
18. Mazur E, Kulik I, Hajný J, Friml J. Auxin canalization and vascular tissue formation by TIR1/AFB-mediated auxin signaling in Arabidopsis. New Phytol. 2020; 226:1375–1383. [PubMed: 31971254]
19. Geldner N, Friml J, Stierhof Y-D, Jürgens G, Palme K. Auxin transport inhibitors block PIN1 cycling and vesicle trafficking. Nature. 2001; 413:425–428. [PubMed: 11574889]

References into the Supplemental Figure

20. Okushima Y, Fukaki H, Onoda M, Theologis A, Tasaka M. ARF7 and ARF19 Regulate Lateral Root Formation via Direct Activation of LBD/ASL Genes in Arabidopsis. Plant Cell. 2007; 19:118–130. [PubMed: 17259263]
21. Knox K, Grierson CS, Leyser O. AXR3 and SHY2 interact to regulate root hair development. Development. 2003; 130:5769–5777. [PubMed: 14534134]
22. Friml J, Wiśniewska J, Benková E, Mendgen K, Palme K. Lateral relocation of auxin efflux regulator PIN3 mediates tropism in Arabidopsis. Nature. 2002; 415:806–809. [PubMed: 11845211]
23. Cecchini NM, Steffes K, Schläppi MR, Gifford AN, Greenberg JT. Arabidopsis AZI1 family proteins mediate signal mobilization for systemic defence priming. Nat Commun. 2015; 6:1–12.
24. Grunewald W, Karimi M, Wieczorek K, Van de Cappelle E, Wischnitzki E, Grundler F, Inze D, Beeckman T, Gheysen G. A Role for AtWRKY23 in Feeding Site Establishment of Plant-Parasitic Nematodes. PLANT Physiol. 2008; 148:358–368. [PubMed: 18599655]
25. Xu J, Scheres B. Dissection of Arabidopsis ADP-RIBOSYLATION FACTOR 1 Function in Epidermal Cell Polarity. Plant Cell. 2005; 17:525–536. [PubMed: 15659621]
26. Wu Y, Xun Q, Guo Y, Zhang J, Cheng K, Shi T, He K, Hou S, Gou X, Li J. Genome-Wide Expression Pattern Analyses of the Arabidopsis Leucine-Rich Repeat Receptor-Like Kinases. Mol Plant. 2016; 9:289–300. [PubMed: 26712505]
27. Irizarry RA, Hobbs B, Collin F, Beazer-Barclay YD, Antonellis KJ, Scherf U, Speed TP. Exploration, normalization, and summaries of high density oligonucleotide array probe level data. Biostatistics. 2003; 4:249–264. [PubMed: 12925520]
28. Saeed AI, Sharov V, White J, Li J, Liang W, Bhagabati N, Braisted J, Klapa M, Currier T, Thiagarajan M, Sturn A, et al. TM4: a free, open-source system for microarray data management and analysis. BioTechniques. 2003; 34:374–378. [PubMed: 12613259]

29. Vanneste S. Cell Cycle Progression in the Pericycle Is Not Sufficient for SOLITARY ROOT/IAA14-Mediated Lateral Root Initiation in Arabidopsis thaliana. PLANT CELL ONLINE. 2005; 17:3035–3050.
30. Karimi M, Depicker A, Hilson P. Recombinational Cloning with Plant Gateway Vectors. Plant Physiol. 2007; 145:1144–1154. [PubMed: 18056864]
31. Tan S, Zhang X, Kong W, Yang X-L, Molnár G, Friml J, Xue H-W. A lipid code-dependent phosphoswitch directs PIN-mediated auxin efflux in Arabidopsis development. bioRxiv. 2019
32. Jia W, Li B, Li S, Liang Y, Wu X, Ma M, Wang J, Gao J, Cai Y, Zhang Y, Wang Y, et al. Mitogen-Activated Protein Kinase Cascade MKK7-MPK6 Plays Important Roles in Plant Development and Regulates Shoot Branching by Phosphorylating PIN1 in Arabidopsis. PLoS Biol. 2016; 14doi: 10.1371/journal.pbio.1002550
33. De Rybel B, Möller B, Yoshida S, Grabowicz I, Barbier de Reuille P, Boeren S, Smith RS, Borst JW, Weijers D. A bHLH Complex Controls Embryonic Vascular Tissue Establishment and Indeterminate Growth in Arabidopsis. Dev Cell. 2013; 24:426–437. [PubMed: 23415953]
34. Wendrich, JR, Boeren, S, Möller, BK, Weijers, D, Rybel, BD. Plant HormonesMethods in Molecular Biology. Humana Press; New York, NY: 2017. 147–158.
35. Tejos R, Sauer M, Vanneste S, Palacios-Gomez M, Li H, Heilmann M, van Wijk R, Vermeer JEM, Heilmann I, Munnik T, Friml J. Bipolar Plasma Membrane Distribution of Phosphoinositides and Their Requirement for Auxin-Mediated Cell Polarity and Patterning in Arabidopsis. Plant Cell. 2014; 26:2114–2128. [PubMed: 24876254]
36. Sauer, M, Friml, J. Plant Developmental Biology: Methods and ProtocolsMethods in Molecular Biology. Hennig, L, Köhler, C, editors. Humana Press; Totowa, NJ: 2010. 253–263.
37. Grones P, Chen X, Simon S, Kaufmann WA, De Rycke R, Nodzyński T, Zažímalová E, Friml J. Auxin-binding pocket of ABP1 is crucial for its gain-of-function cellular and developmental roles. J Exp Bot. 2015; 66:5055–5065. [PubMed: 25922490]
38. Schindelin J, Arganda-Carreras I, Frise E, Kaynig V, Longair M, Pietzsch T, Preibisch S, Rueden C, Saalfeld S, Schmid B, Tinevez J-Y, et al. Fiji: an open-source platform for biological-image analysis. Nat Methods. 2012; 9:676–682. [PubMed: 22743772]
39. Vera-Sirera F, De Rybel B, Úrbez C, Kouklas E, Pesquera M, Álvarez-Mahecha JC, Minguet EG, Tuominen H, Carbonell J, Borst JW, Weijers D, et al. A bHLH-Based Feedback Loop Restricts Vascular Cell Proliferation in Plants. Dev Cell. 2015; 35:432–443. [PubMed: 26609958]
40. Gehl C, Waadt R, Kudla J, Mendel R-R, Hänsch R. New GATEWAY vectors for high throughput analyses of protein-protein interactions by bimolecular fluorescence complementation. Mol Plant. 2009; 2:1051–1058. [PubMed: 19825679]
41. Schütze K, Harter K, Chaban C. Bimolecular fluorescence complementation (BiFC) to study protein-protein interactions in living plant cells. Methods Mol Biol Clifton NJ. 2009; 479:189–202.
42. Thompson JD, Gibson TJ, Plewniak F, Jeanmougin F, Higgins DG. The CLUSTAL_X windows interface: flexible strategies for multiple sequence alignment aided by quality analysis tools. Nucleic Acids Res. 1997; 25:4876–4882. [PubMed: 9396791]
43. Kumar S, Stecher G, Tamura K. MEGA7: Molecular Evolutionary Genetics Analysis Version 7.0 for Bigger Datasets. Mol Biol Evol. 2016; 33:1870–1874. [PubMed: 27004904]
44. Sierla M, Hõrak H, Overmyer K, Waszczak C, Yarmolinsky D, Maierhofer T, Vainonen JP, Salojärvi J, Denessiouk K, Laanemets K, Tõldsepp K, et al. The Receptor-like Pseudokinase GHR1 Is Required for Stomatal Closure. Plant Cell. 2018; 30:2813–2837. [PubMed: 30361234]
45. Langeberg LK, Scott JD. Signalling scaffolds and local organization of cellular behaviour. Nat Rev Mol Cell Biol. 2015; 16:232–244. [PubMed: 25785716]

Europe PMC Funders Author Manuscripts

One Sentence Summary

An auxin-responsive receptor-like kinase complex regulates directional auxin transport

Europe PMC Funders Author Manuscripts

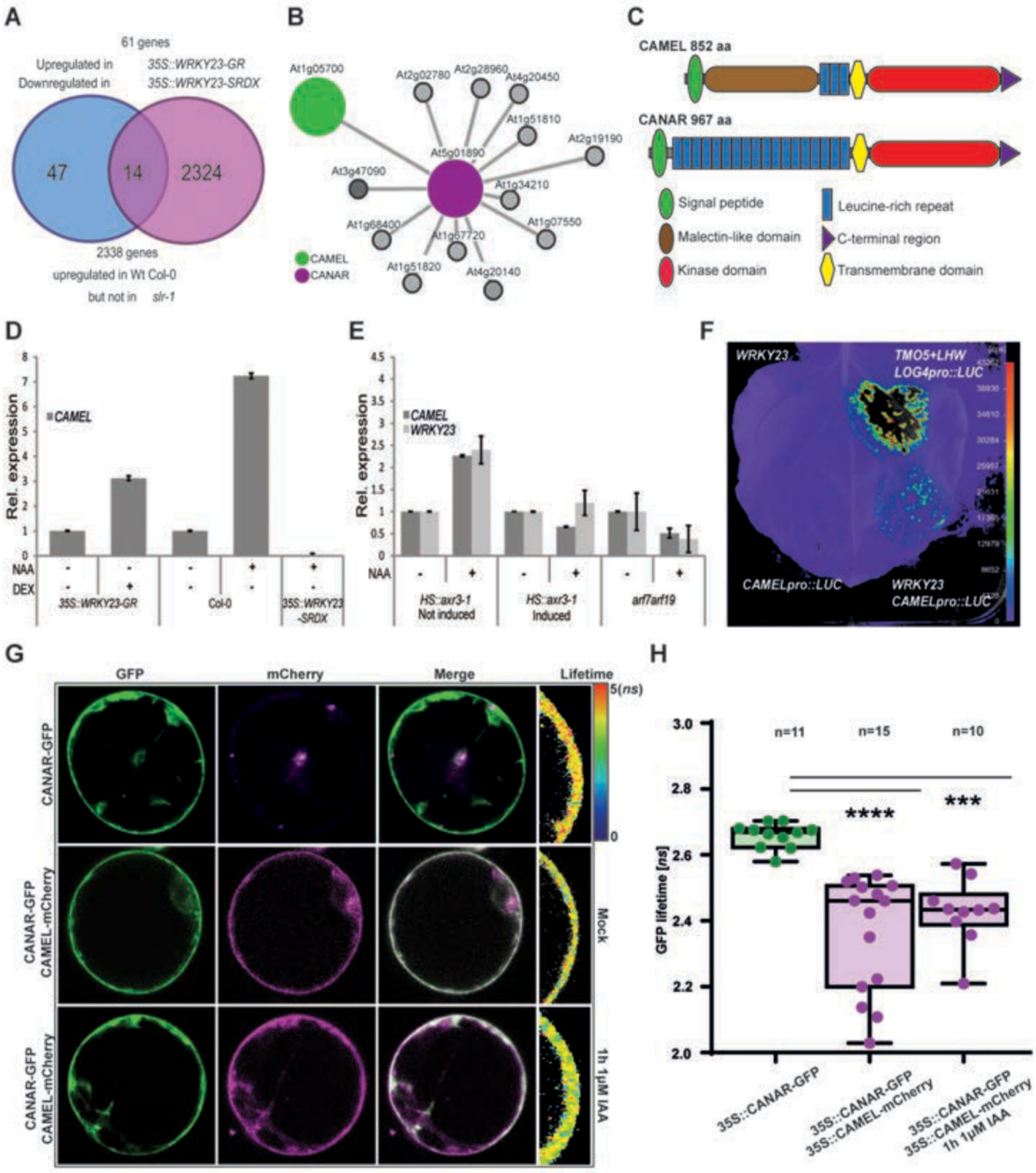

Fig. 1. *CAMEL* expression is regulated by WRKY23 and depends on the TIR1/AFB pathway.

(**A**) Scheme of the microarray experimental setup to identify auxin-regulated genes downstream of the TIR1/AFB-WRKY23 signaling module.

(**B**) Map of physical interactions between extracellular domains of putative interactors of CANAR from a previous study (16) with CAMEL being one of high confidence, illustrated with the BAR interaction viewer.

(**C**) Schematic representation of the domain organization of CAMEL and CANAR.

Europe PMC Funders Author Manuscripts

(**D** and **E**) RT-qPCR experiments showing that **(D)** *CAMEL* expression depends on WRKY23 and **(E)** auxin-mediated upregulation of *CAMEL* requires the TIR1/AFB activity.
(**F**) Luciferase assay in *Nicotiana benthamiana: 35S::WRKY23* co-expressed with *CAMELpro:LUC* and negative control of *35S:WRKY23* or *CAMAL:LUC* was indicated respectively.
(**G** and **H**) FRET-FLIM analysis of transiently expressed *35S::CANAR-GFP* and *35S::CAMEL-mCherry* in protoplasts. The GFP fluorescence lifetime was calculated as described in the Methods section and the heat map represents the fluorescent lifetime values. A One-Way ANOVA test compared marked sets of data (***, $p<0.001$; ****, $p<0.0001$). *n* denotes the number of scored protoplasts.

Europe PMC Funders Author Manuscripts

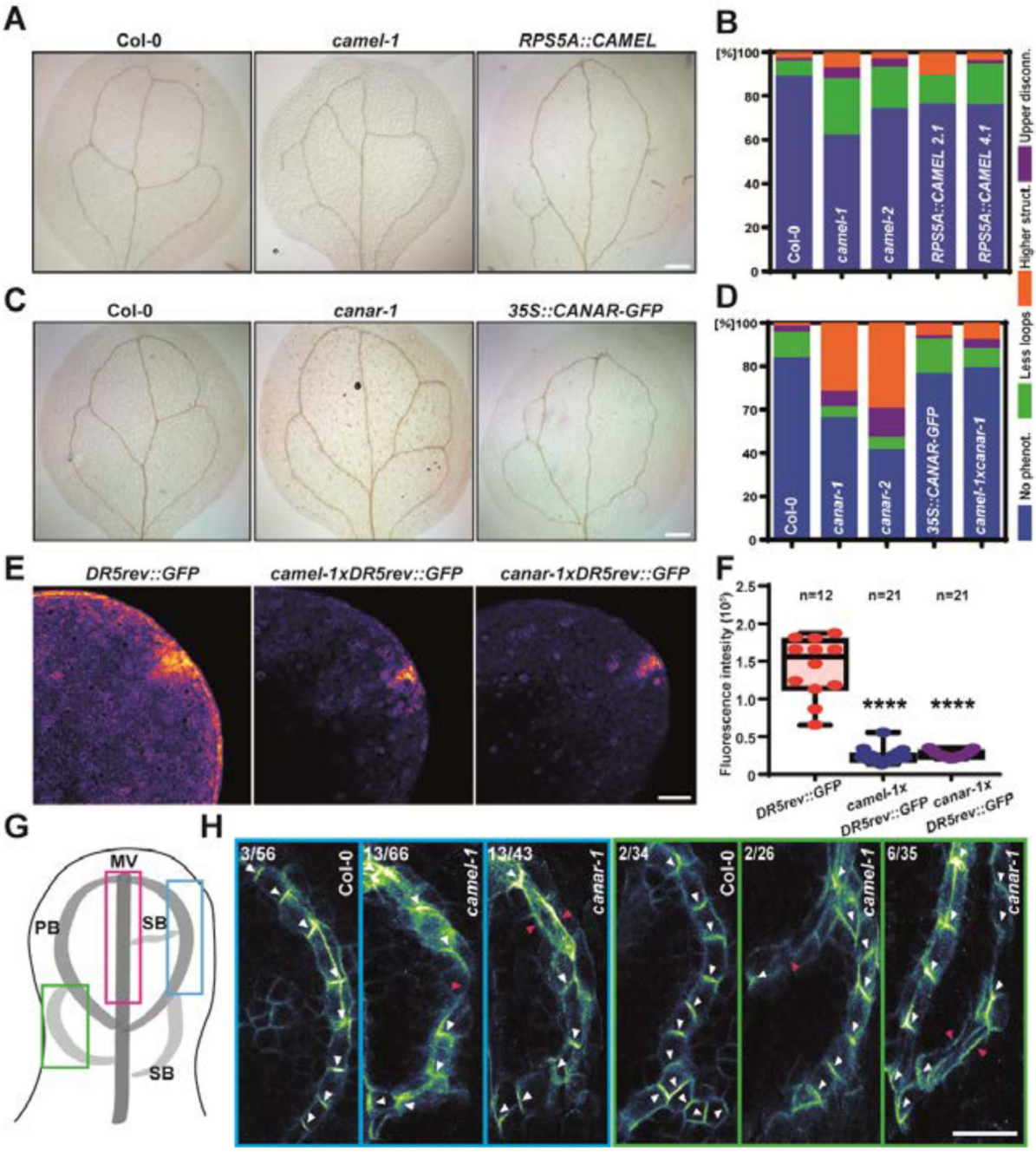

Fig. 2. Abnormal patterning and PIN1 polarization during leave venation in *camel* and *canar* mutants

(**A** and **C**) Representative images of venation patterning defects in cotyledons associated with *camel-1* **(A)** or *canar-1* **(C)**, respectively. Scale bar: 100 μm.

(**B** and **D**) Quantification of venation defects in *camel* and *canar* mutants (n>75 for each genotype). Scored categories: No phenotype, less loops, higher structure (including extra loops or branches) and upper disconnections.

(**E** and **F**) *DR5rev::GFP* signal distribution and **(F)** intensity in cotyledons of *camel-1*/*canar-1* mutants. (n>12 for each genotype). Scale bar: 100 μm.
(**G** and **H**) Coordinated PIN1 polarity in Col-0 and defective PIN1 polarity in *camel-1*/*canar-1* mutants. Colored boxes in **(G)** illustrate positions of close-ups in **(H)**. **(H)** Representative images of PIN1 immunolocalization in firstleaves. A number in left top corner indicates an incidence of observed PIN1 defective polarity to a total amount of analyzed leaves. White arrows show a typical PIN1 polar localization. Red arrows mark a defective PIN1 polarity. Evaluation criteria are described in Material and Method section. Scale bar: 10 μm

Europe PMC Funders Author Manuscripts

Europe PMC Funders Author Manuscripts

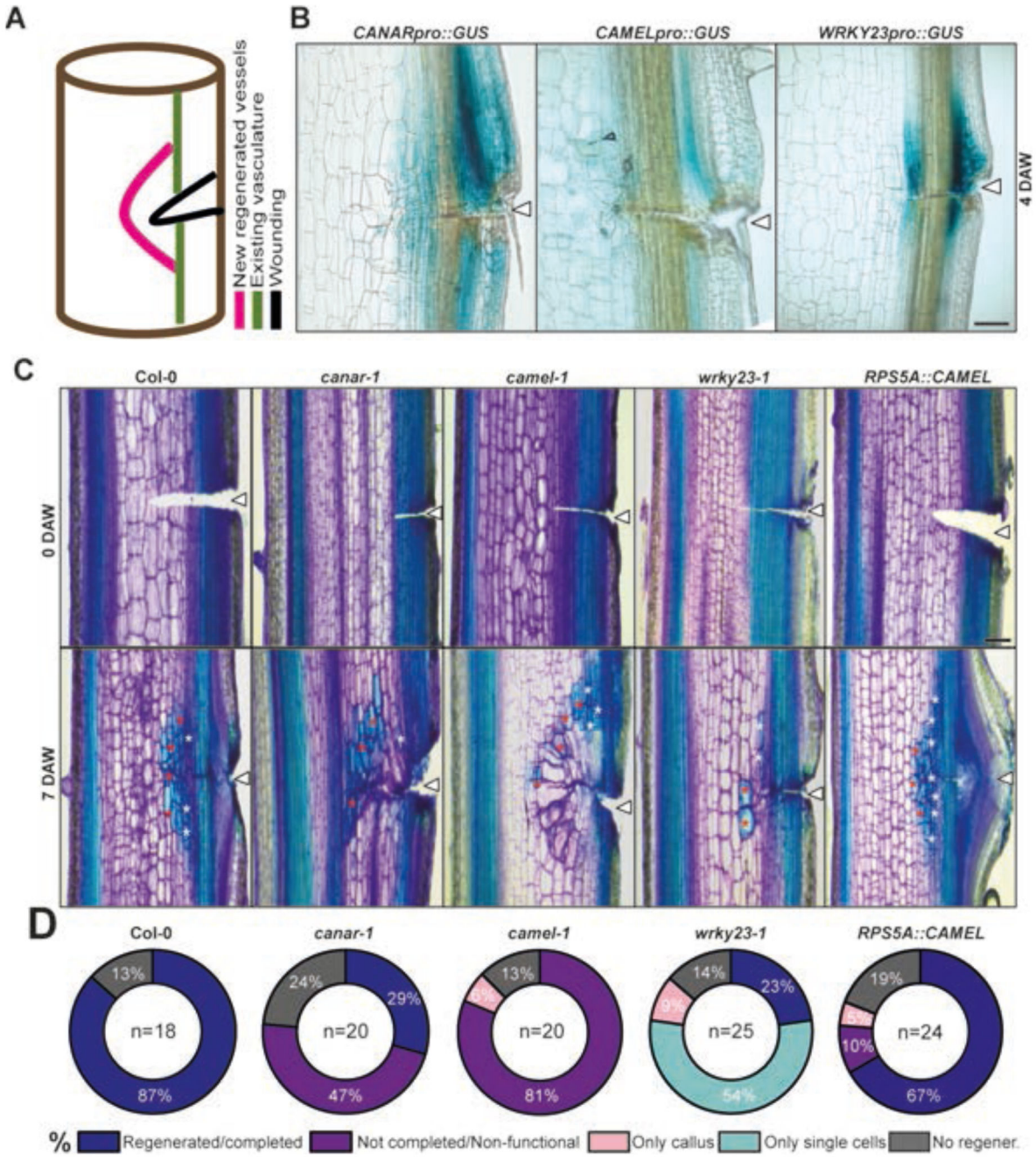

Fig. 3. Defective vasculature regeneration after wounding in *camel*, *canar* and *wrky23-1* mutants.

(**A**) Scheme of the experiment for analyzing vasculature regeneration after wounding.

(**B**) Expression of *CANARpro::GUS, CAMELpro::GUS* and *WRKY23pro::GUS* 4 days after wounding (DAW). The wound site is marked by a white arrowhead. Scale bar: 100 μm.

(**C**) Wounded stems of *canar-1, camel-1, wrky23-1* mutants and *RPS5A::CAMEL* overexpressing line at 0 and 7 DAW. Stems are stained by toluidine blue to visualize newly regenerated blue-vessel cells (white asterisks) and lignified parenchyma cells (red asterisks). The wound site is marked by a white arrowhead.

(**D**) Quantification of regeneration defects in **(C)**. *n* denotes the number of evaluated plants. Scale bar: 100 μm.

Europe PMC Funders Author Manuscripts

Europe PMC Funders Author Manuscripts

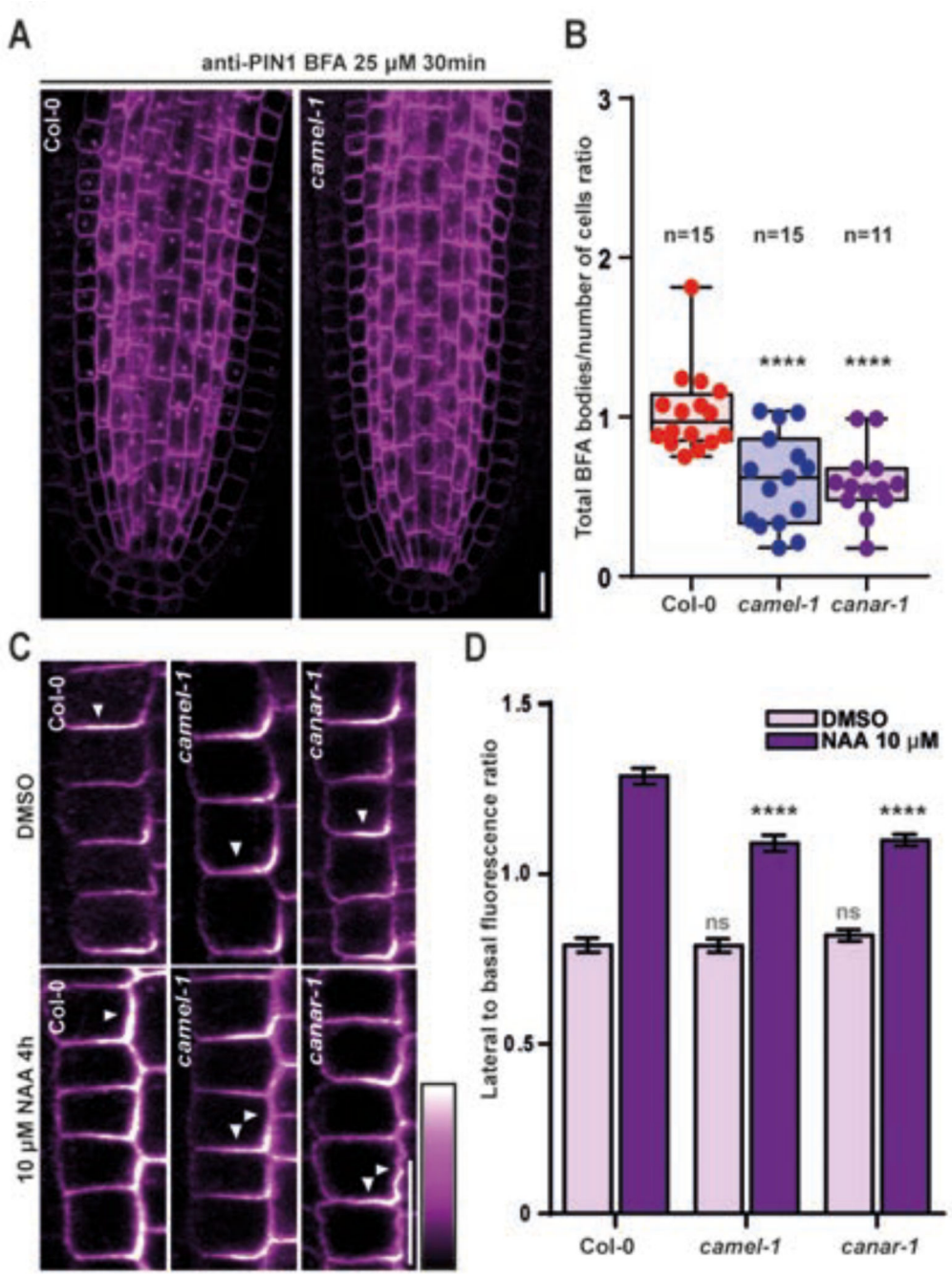

Fig. 4. Subcellular trafficking and auxin feed-back on PIN polarity is compromised in *camel* and *canar* mutants.

(**A**) Representative confocal images of primary root stele cells after immunostaining PIN1 in Wt, *camel-1* and *canar-1*. Seedlings were BFA-treated (25µM) for 30min. Scale bar: 10 µm.

(**B**) Quantitative evaluation of **(A)** shows ratio of total number of BFA bodies/total number of cells per root. *n* denotes the number of evaluated seedlings (****p<0.0001).

(**C**) Immunolocalization of PIN1 in endodermis of root meristem after 4h NAA (10µM) treatment. Scale bar: 10 µm.

(**D**) Quantitative evaluation of **(C)** shows mean ratio of PIN1 lateral-to-basal signal intensity ratio in endodermal cells. Error bars indicate standard error. The experiment was carried out three times, one representative experiment is presented. A One-Way ANOVA test compared marked datasets (****$p<0.0001$; $n>80$ cells corresponding to a minimum of 10 roots per treatment and experiments were imaged using comparable settings).

Europe PMC Funders Author Manuscripts

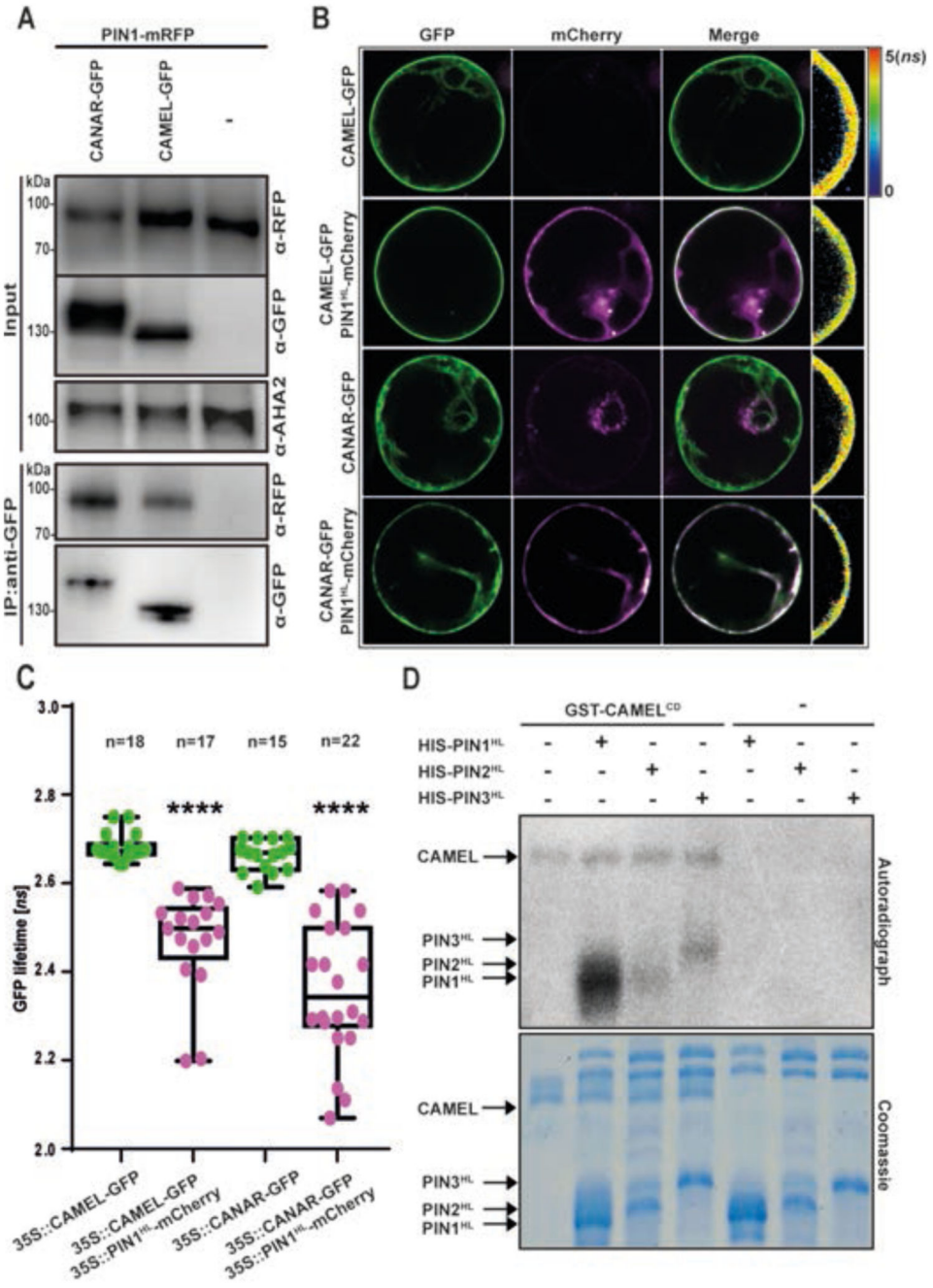

Fig. 5. The CAMEL-CANAR signaling module directly targets PIN1.

(**A**) Co-immunoprecipitation (Co-IP) assay from *Arabidopsis* root protoplasts. The protein complex of CAMEL-PIN1 and CANAR-PIN1 was co-immunoprecipitated by anti-GFP beads. Anti-AHA2 was used as loading control. The experiment was carried out three times. (**B** and **C**) FRET-FLIM analysis of transiently expressed *35S::CAMEL-GFP* and *35S::CANAR-GFP* with *35S::PIN1^{HL}-mCherry* (HL-hydrophilic loop) in protoplasts. The GFP fluorescence lifetime was calculated as described in the Methods section and the heat

map indicates fluorescent lifetime values. A One-Way ANOVA test compared the marked data sets (****, $p<0.0001$). *n* denotes the number of scored protoplasts.
(**D**) Autoradiograph of an *in vitro* kinase phosphorylation assay of $PIN1/2/3^{HL}$ by $CAMEL^{CD}$ (CD-cytoplasmic domain). Aliquots of the samples were separated by SDS-PAGE and exposed to autoradiography. The coomassie blue staining was used as loading control and presence of the respective recombinant proteins. The blots shown are representative for three biological replicates.

Europe PMC Funders Author Manuscripts

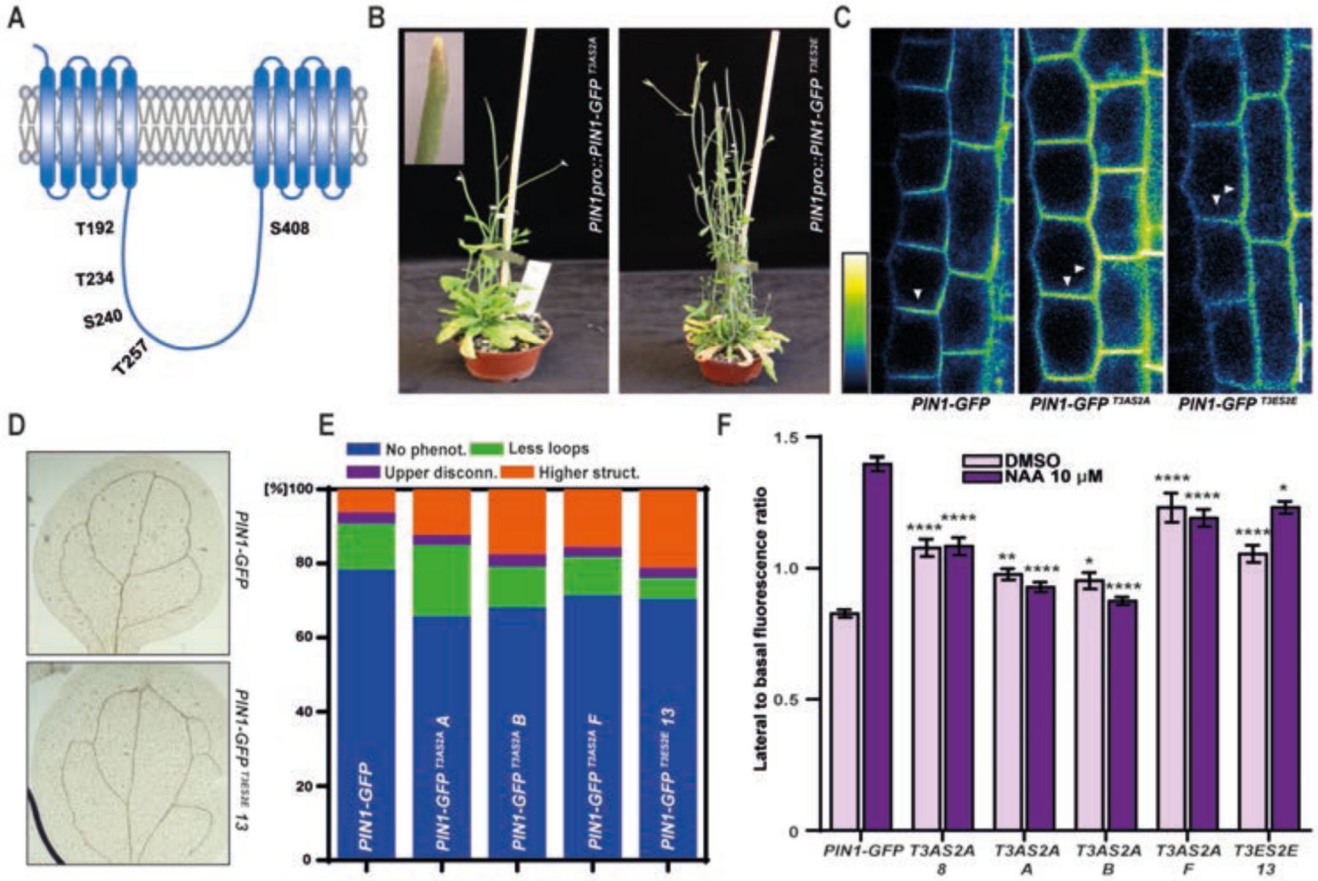

Fig. 6. CAMEL-targeted phosphosites in the PIN1 cytoplasmic loop are important for PIN polarity and venation.

(**A**) Schematic representation of PIN1 in the plasma membrane with marked positions of phosphosites in the cytoplasmic loop targeted by CAMEL.

(**B**) Phenotypes of *PIN1pro::PIN1-GFP*^{T3AS2A} and *PIN1pro::PIN1-GFP*^{T3ES2E}. 35 days old.

(**C**) Subcellular localization of PIN1-GFP, PIN1-GFP^{T3AS2A} and PIN1-GFP^{T3ES2E} in root meristem endodermal cells. White arrows mark the predominant subcellular localization.

(**D**) Representative images of vasculature defects in cotyledons of *PIN1pro::PIN1-GFP*, *PIN1pro::PIN1-GFP*^{T3ES2E} (line13). Scale bar: 100 µm.

(**E**) Quantification of vasculature defects in *PIN1pro::PIN1-GFP*, *PIN1pro::PIN1-GFP*^{T3AS2A} (lines A, B, F) and *PIN1pro::PIN1-GFP*^{T3ES2E} (line 13) (n>68 for each genotype). Scored categories: normal vasculature, less loops, higher structure (including extra loops or branches) and upper disconnections.

(**F**) Quantitative evaluation of (Fig. S6D) shows the mean lateral-to-basal ratio of PIN1-GFP signal in endodermal cells. Error bars indicate standard errors. The experiment was carried out three times, one representative experiment is presented. A One-Way ANOVA test was performed to compare marked datasets (*p<0.05,**p<0.01,***p<0.001,****p<0.0001; n>40 cells corresponding to a minimum of 8 roots per treatment and experiments were imaged using comparable settings).

Europe PMC Funders Author Manuscripts